Bioorganic Chemistry 87 (2019) 655–666

Contents lists available at ScienceDirect

Bioorganic Chemistry

journal homepage: www.elsevier.com/locate/bioorg

Design and synthesis of novel PARP-1 inhibitors based on pyridopyridazinone scaffold

Ghada F. Elmasry*, Enayat E. Aly, Fadi M. Awadallah, Samir M. El-Moghazy

Department of Pharmaceutical Chemistry, Faculty of Pharmacy, Cairo University, El-Kasr El-Eini Street, P.O. Box 11562, Cairo, Egypt

ARTICLE INFO

Keywords:
Pyridopyridazinones
PARP-1 inhibitors
Olaparib
Molecular docking

ABSTRACT

Various pyridopyridazinone derivatives were designed as Poly(ADP-ribose) polymerase-1 (PARP-1) inhibitors. The pyridopyridazinone scaffold was used as an isostere of the phthalazine nucleus of the lead compound Olaparib in addition to some modifications in the tail part of the molecule. Preliminary biological evaluation indicated that most compounds possessed inhibitory potencies comparable to Olaparib in nanomolar level. The best PARP-1 inhibitory activity was observed for compound **8a** with (IC_{50} = 36 nM) compared to Olaparib as a reference drug (IC_{50} = 34 nM). Molecular modeling simulation revealed that, the designed compounds docked well into PARP-1 active site and their complexes are stabilized by three key hydrogen bond interactions with both Gly863 and Ser904 as well as other favorable π-π and hydrogen-π stacking interactions with Tyr907 and Tyr896, respectively. Computational ADME study predicted that the target compounds **8a** and **8e** have proper pharmacokinetic and drug-likeness properties. These outcomes afford a new structural framework for the design of novel inhibitors for PARP-1.

1. Introduction

Cancer is a disease characterized by uncontrolled growth of abnormal cells disregarding the normal cell division rules. Normal cells are continually subject to signals that regulate the cell division, differentiation or death. Cancer cells deregulate these signals, leading to uncontrolled division and proliferation [1].

Poly(ADP-ribose) polymerase (PARP) inhibitors represent an interesting novel class of targeted cancer therapies [2,3]. Poly(ADP-ribose) polymerase-1 (PARP-1) is a chromatin-bound nuclear enzyme capable of DNA repair as it recognizes and binds rapidly to DNA single or double strand breaks [4,5]. Activated PARP-1 utilizes NADP to synthesize poly (ADP)-ribose upon association with DNA, either on itself or on a variety of nuclear target proteins such as histones, topoisomerases, DNA ligases and DNA polymerases [6,7]. This leads to the formation of highly negatively charged nuclear proteins that facilitate the recruitment of the damaged DNA through the base excision repair (BER) machinery. Thus, inhibition of PARP enhances the effects of cytotoxic drugs such as topoisomerase I inhibitors and DNA alkylating agents as well as ionizing radiation [8,9]. Furthermore, some PARP inhibitors have been shown to display single agent activity against tumors exhibiting BRCA1- or BRCA2-mutations [10,11]. Accordingly, development of PARP inhibitors is an attractive research area providing advanced cancer treatment possibilities.

Few PARP-1 inhibitors have been discovered and FDA approved e.g., Olaparib **II** [12], Niraparib **III** [13], Rucaparib **IV** [14] and Talazoparib **V** [15]. Moreover, several phthalazinones have been considered as effective orally bioavailable PARP inhibitors [16,17] such as KU58948 **VI** and AZD 2461 **VII** (Fig. 1).

Nevertheless, effort of pursuing new inhibitors with high potency, significant aqueous solubility and good oral bioavailability against PARP-1 is still needed.

Surveying the literature revealed that the design of PARP-1 inhibitors generally depends on the nicotinamide moiety of NAD+ to mimic the ligand-protein interaction of NAD+ with PARP-1 [18] and thus the common pharmacophoric features are aromatic ring and carboxamide moiety, which can form hydrogen bonds and π-stacking interactions in PARP-1 catalytic domain [19–21].

X-Ray crystal structures of PARP-1 with bound inhibitors [22] and molecular modeling studies [20,23] indicate that there are three crucial hydrogen bond interactions between the carboxamide moiety and two critical amino acid residues in the PARP active site, Gly863 (NH to Gly C=O and C=O to Gly NH) and Ser904 (C=O to Ser OH). In addition, the phenyl moiety of Tyr907 makes π-π stacking interaction with the nicotinamide of NAD+. Attempts to improve PARP inhibitors' binding affinity have been made by restriction of the carboxamide group which is usually free to rotate. Locking of the carboxamide group into the required conformation can be made by either inserting on the aromatic

* Corresponding author.
E-mail address: ghada.elmasry@pharma.cu.edu.eg (G.F. Elmasry).

https://doi.org/10.1016/j.bioorg.2019.03.068
Received 25 February 2019; Received in revised form 24 March 2019; Accepted 25 March 2019
Available online 28 March 2019
0045-2068/

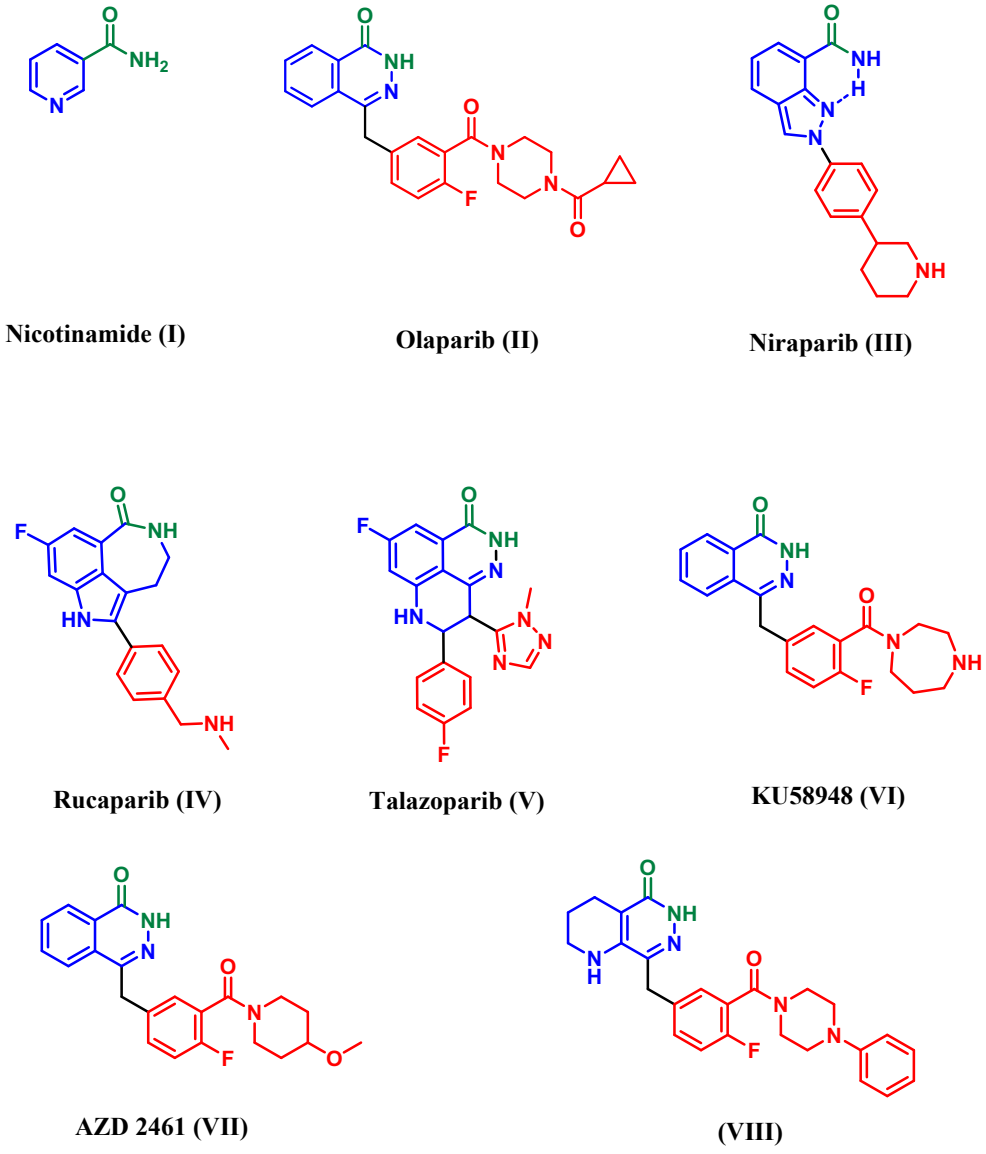

Fig. 1. Nicotinamide-based PARP-1 inhibitors.

ring heteroatoms or groups able to give an intramolecular hydrogen bond with the amide NH, or enclosing the amide group into a bicyclic system [19].

Based on these findings, the design of the new compounds relied on the use of the phthalazinone derivatives (**II**, **VI** and **VII**) as lead compounds where two main modifications were conducted. The first structural modification involved an isosteric replacement of the phthalazinone nucleus with the pyridopyridazinone scaffold. Literature review revealed that the majority of PARP-1 inhibitors are phthalazinones, quinazolinones or isoquinolinones [24,25], and to our knowledge none of them featured the nicotinamide moiety i.e. the pyridine ring and the carboxamide group (in the form of lactam) at its 3-position. This urged us to mimic the nicotinamide moiety and incorporate it as a bicyclic system namely, pyridopyridazine. This also aimed to maintain low lipid solubility and blood brain barrier permeability similar to Olaparib to avoid possible penetration and CNS side effects [26,27]. In silico pharmacokinetic study proved that if our compounds possessed a phthalazinone instead of the pyridopyridazinone nucleus they would have high blood brain barrier penetration. Moreover, it was reported that the presence of nitrogen in the tetrahydro-pyridopyridazinone scaffold of compound **VIII** improved the pharmacokinetic properties over similar carbon based analogues [20]. The second structural modification pertained to attaching a variety of functional pharmacophoric fragments to the pendant benzyl group at position 4 of the pyridopyridazinone scaffold. These fragments were attached through an amide linkage at position 4 of the benzyl group to block possible metabolism at this position and extend half-life.

In summary, the current design featured the following pharmacophoric elements: (1) a hetero aromatic ring (pyridyl ring was taken instead of phenyl of the phthalazinone to mimic the nicotinamide moiety, seek new possibilities and explore alternative chemical templates), (2) a lactam moiety with NH group locked into the required conformation, this was achieved with ring closure of the carboxamide into bicyclic system, (3) an auxiliary appendage with a shorter or longer chain is generally attached to the polycyclic core as a solvent accessory region (the substitutions at the para position of benzyl contribute to block possible metabolism and extend half-life) [17] as shown in Fig. 2.

To verify the rationale of the design and to approach the development of potent inhibitors, the molecular docking study of all of the compounds to the catalytic domain of PARP-1 was first conducted. Affinity of the compounds to the target enzyme was judged by comparing the binding free energy (docking score) and the binding mode of the target compounds with that of the co-crystallized ligand Olaparib. Analysis of the docking results showed that all the designed compounds

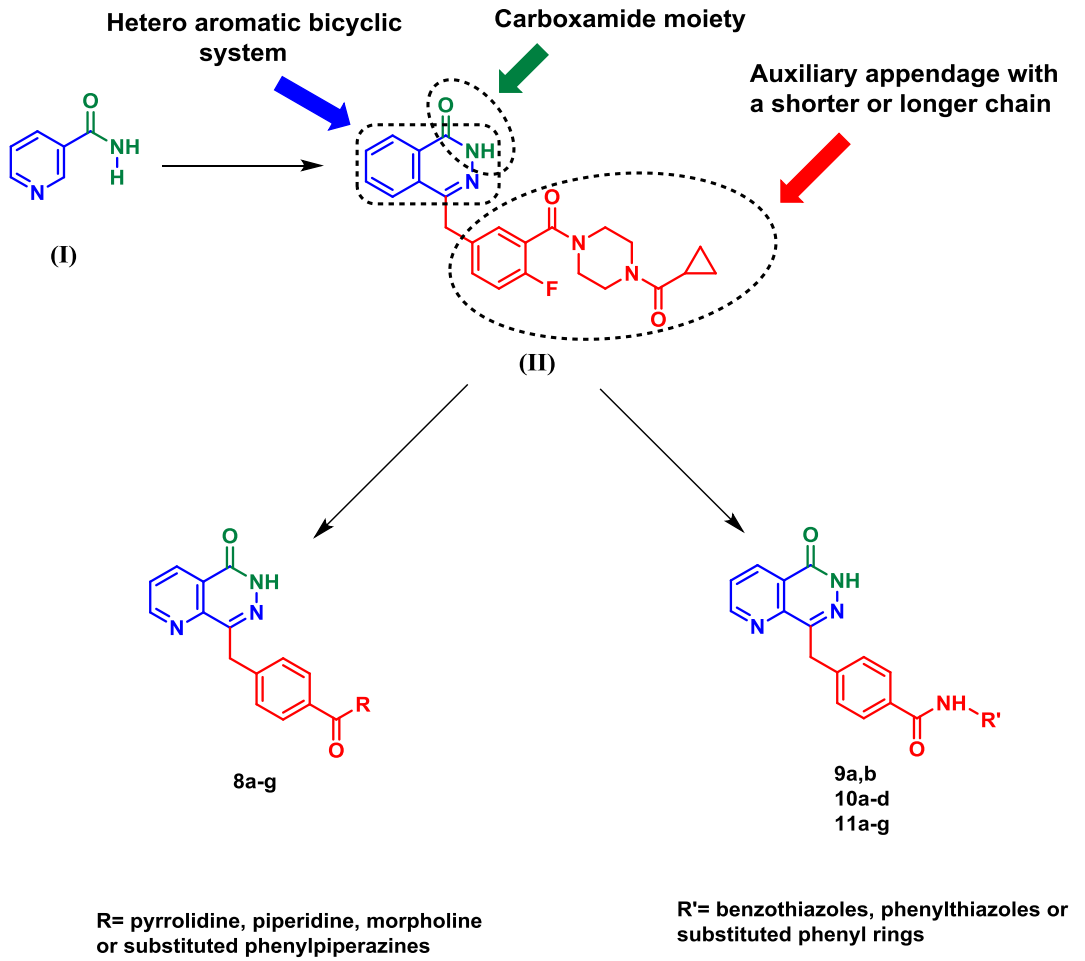

Fig. 2. Design approach of the targeted pyridopyridazinone derivatives **8a-g**, **9a and b**, **10a-d** and **11a-g** as PARP-1 inhibitors.

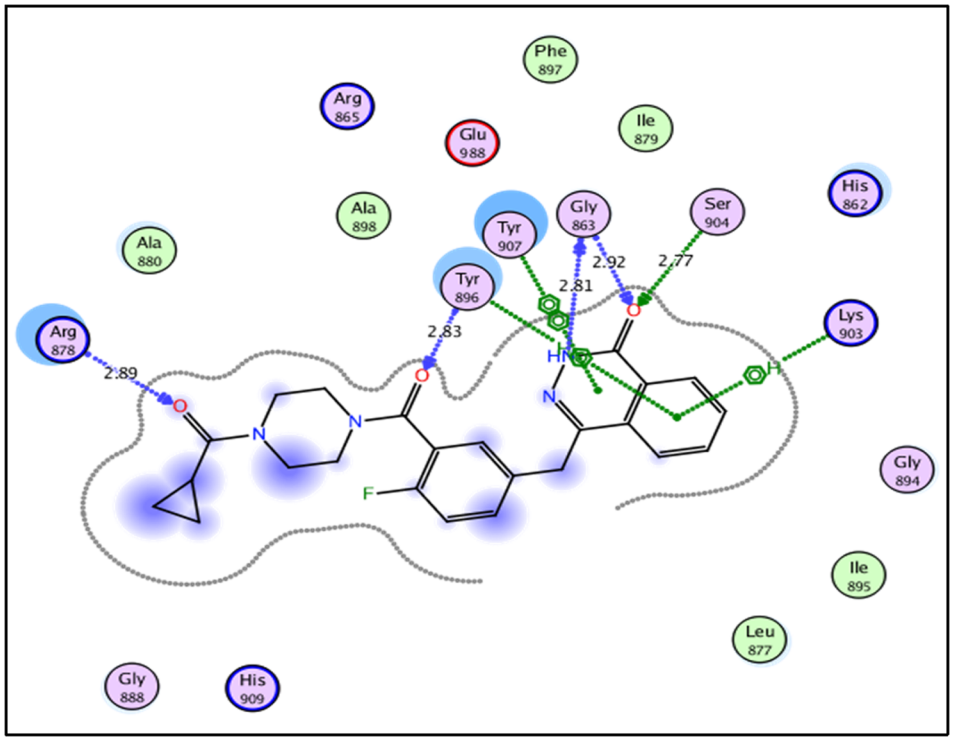

Fig. 3. 2D interaction diagram showing Olaparib docking pose interactions with the key amino acids in the PARP-1 active site (distances in Å).

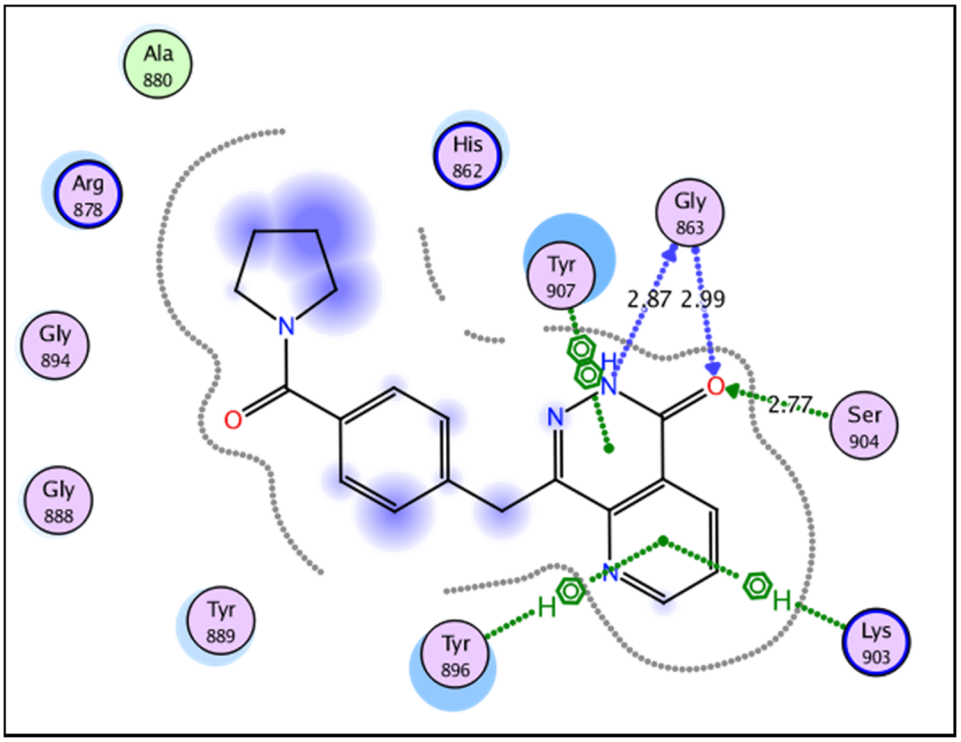

Fig. 4. 2D diagram of compound **8a** showing its interactions with the PARP-1 active site (distances in Å).

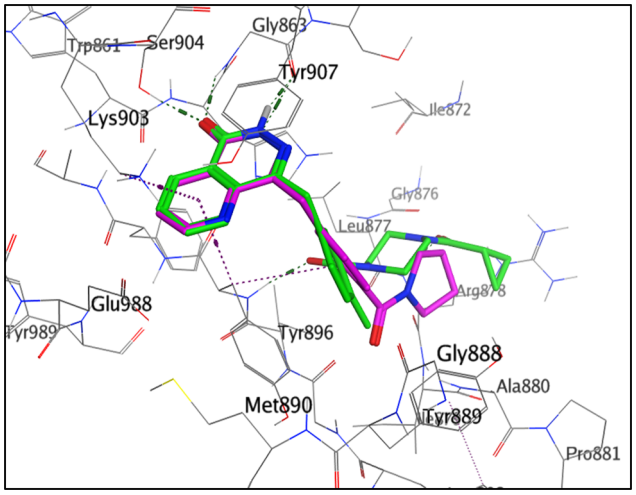

Fig. 5. X-Ray Co-crystal structure of Olaparib (green) overlaid with the proposed binding mode of compound **8a** (magenta) in the catalytic domain of human PARP-1 showing the main interactions with the key amino acids in the active site.

fit into the active site of PARP-1, most of them displayed comparable docking scores and binding modes similar to that of Olaparib and were able to reproduce all the main interactions accomplished by the co-crystallized ligand with the key amino acids in the active site. Docking of Olaparib, docking of compound **8a**, and alignment of the co-crystallized ligand (Olaparib) and compound **8a** in the catalytic domain of human PARP-1 are shown in Figs. 3–5.

2. Results and discussion

2.1. Chemistry

The new pyridopyridazinone derivatives were synthesized, as depicted in Schemes 1 and 2. At first, the quinolinic anhydride **2** was prepared as reported by the reaction of acetic anhydride with quinolinic acid **1** [28,29]. Next, reduction of quinolinic anhydride with $NaBH_4$ in dry tetrahydrofuran in the presence of acetic acid was done to obtain the intermediate 2-hydroxymethyl-3-pyridinecarboxylic acid **3**, which spontaneously lactonized upon addition of acetic anhydride to yield the furo[3,4-*b*]pyridin-5(7*H*)-one **4** [32,33]. Reaction of compound **4** with 4-carboxy benzaldehyde using sodium methoxide in methanol and ethyl acetate gave the corresponding 4-(5-hydroxy-7-oxo-7*H*-cyclopenta[*b*]pyridin-6-yl)benzoic acid **5**, which was then reacted with excess hydrazine hydrate at 100 °C to obtain the key compound 4-((5-oxo-5,6-dihydropyrido[2,3-*d*]pyridazin-8-yl)methyl)benzoic acid **6**.

The synthesis of the target compounds is illustrated in Scheme 2 where one pot amide synthesis was adopted in which the acid chloride **7**, obtained from the reaction of the precursor acid derivative **6** with thionyl chloride, was reacted with the appropriate amino compounds *viz*, secondary amines, 2-aminobenzothiazoles, 2-aminophenylthiazoles, anilines and sulfanilamide in dry DMF in the presence of triethylamine to give **8a-g**, **9a and b**, **10a-d** and **11a-g**, respectively. The postulated structures of the products were proved by the disappearance of carboxylic OH band in the IR spectra and its exchangeable signals in the ^{1}H NMR spectra. Furthermore, the ^{1}H NMR showed characteristic signals at δ 1.58–3.41 ppm region attributed to the morpholino, piperidino, pyrrolidino or piperazino protons in compounds **8a-g,** in addition to signals attributed to the additional aromatic protons in compounds **8d-g**. ^{1}H NMR spectra of compounds **9a and b**, **10a-d** and **11a-g** showed additional deuterium exchangeable singlet signals around δ 10.06–10.47 ppm corresponding to the new NH proton, in addition to the aromatic protons signals of the attached moieties. ^{13}C NMR supported the carbon skeleton of the target compounds.

2.2. In vitro PARP-1 inhibitory activity

In order to gain a more clear insight to the structure–activity relationship, all final compounds were evaluated for their inhibitory activity on PARP-1. The IC_{50} values of all the tested compounds against

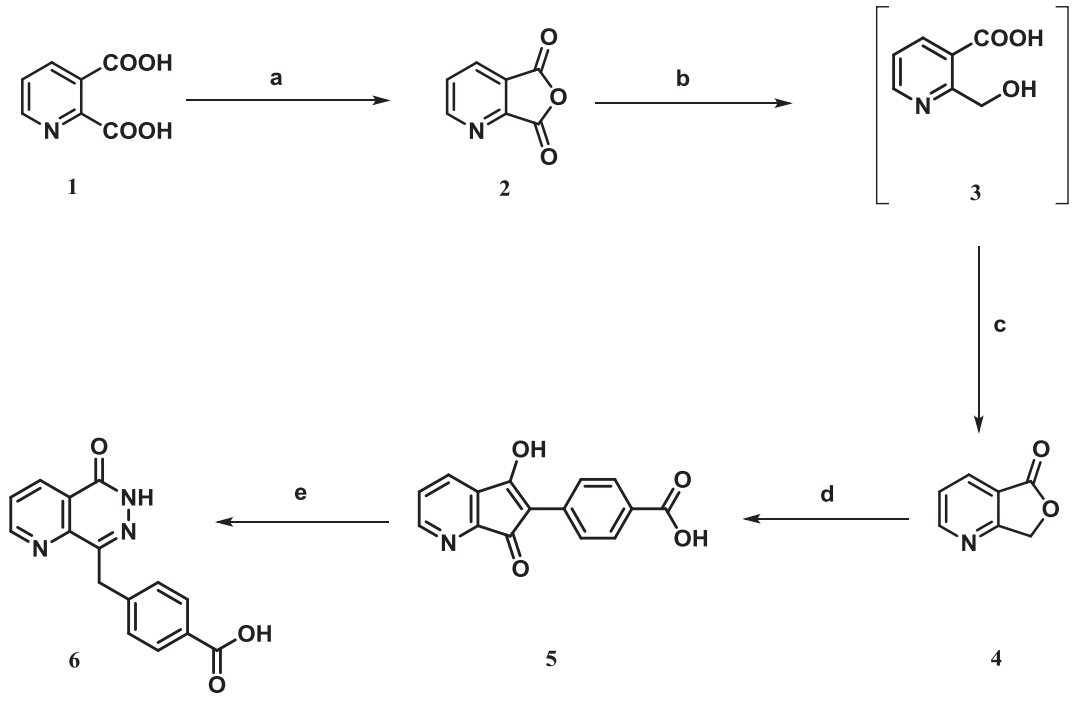

Reagents and solvents: a) acetic anhydride, b) $NaBH_4$, acetic acid, THF, c) acetic anhydride, d) 4-carboxybenzaldehyde, methanol, ethylacetate, e) hydrazine hydrate.

Scheme 1. Preparation of the key starting compound **6**.

PARP-1 expressed in (nM concentration) and pIC_{50} values (-log IC_{50} in molar) compared to the reference drug Olaparib are summarized in Table 1.

Interestingly, the target pyridopyridazinones **8a-g, 9a and b, 10a-d** and **11a-g** exhibited a wide range of PARP-1 inhibitory activity but all in the nanomolar range with IC_{50} in the range of 36–634 nM. It can therefore be claimed that a wide variety of substituents can be tolerated at the terminal position of the molecule. This observation can be rationalized if these side chains are approaching the solvent surface and do not significantly interact with the enzyme. However, it was noted that hydrophobic residues are preferred at this position particularly. Concerning the shorter derivatives **8a-c** of the substituted carbonyl series **8a-g**, the pyrrrolo derivative **8a** was found to be the most active and the order of activity was pyrrolo > piperidino > morpholino. It is worth to mention that **8a** displayed the highest activity among the all the target compounds (IC_{50} = 36 nM) approaching the activity of the control Olaparib (IC_{50} = 34 nM). For the compounds bearing phenyl piperazine moities **8d-g**, introduction of an electron-donating group on the benzene ring increased the inhibitory activity as depicted by the methoxy derivative **8e,** while the electron-withdrawing substituted derivatives (Cl and CF_3) (**8f** and **8g**, IC_{50} = 180 and 142 nM, respectively) displayed much lower potency compared to the unsubstituted analogue (**8d**, IC_{50} = 71 nM). Comparing the benzothiazole derivatives **9a and b** and their phenylthiazole counterparts **10a-d** revealed that the fusion of the thiazole moiety with the phenyl ring did not elicit significant changes in the inhibitory activity. Moreover, substituted and unsubstituted benzothiazole congeners were nearly equipotent. Regarding the phenylthiazole series, the unsubstituted phenylthiazole **10a** derivative showed high potency (IC_{50} = 45 nM). On the contrary, the methyl congener **10b** displayed much lower activity (IC_{50} = 218 nM). Replacement of the methyl group with methoxy or bromo substituents enhanced the activity where compounds **10c** and **10d** showed IC_{50} = 53 and 60 nM, respectively. With respect to the anilino derivatives **11a-f,** the unsubstituted compound **11a** exhibited the lowest activity among all the synthesized compounds. Exploring the effect of different substituents at position 4 on the benzamide moiety, revealed that the introduction of electron donating groups enhanced the inhibitory potency *viz* the hydroxy **11b** and methoxy **11d** derivatives rather than electron withdrawing groups. Finally, the sulfonamide derivative **11g** showed good potency.

3. *In silico* studies

3.1. Molecular docking

The molecular docking approach for all of the compounds was used to support the design hypothesis prior synthesis as mentioned before. Crystallographic structure of the human PARP-1 catalytic domain (PDB code: 5DS3) was obtained from the Protein Data Bank (PDB) database. The key interactions in the PARP-1 active site, consistent with previous literature reports, were highlighted. The lactam amide group of almost all the designed molecules displayed three key hydrogen-bond interactions with both Ser904 and Gly863; which involved the interaction of the pyridazinone carbonyl group as H-bond acceptor with the backbone carbonyl of Gly863 -NH group and Ser904 -OH group, besides the interaction of the pyridazinone ring NH as H-bond donor with Gly863.

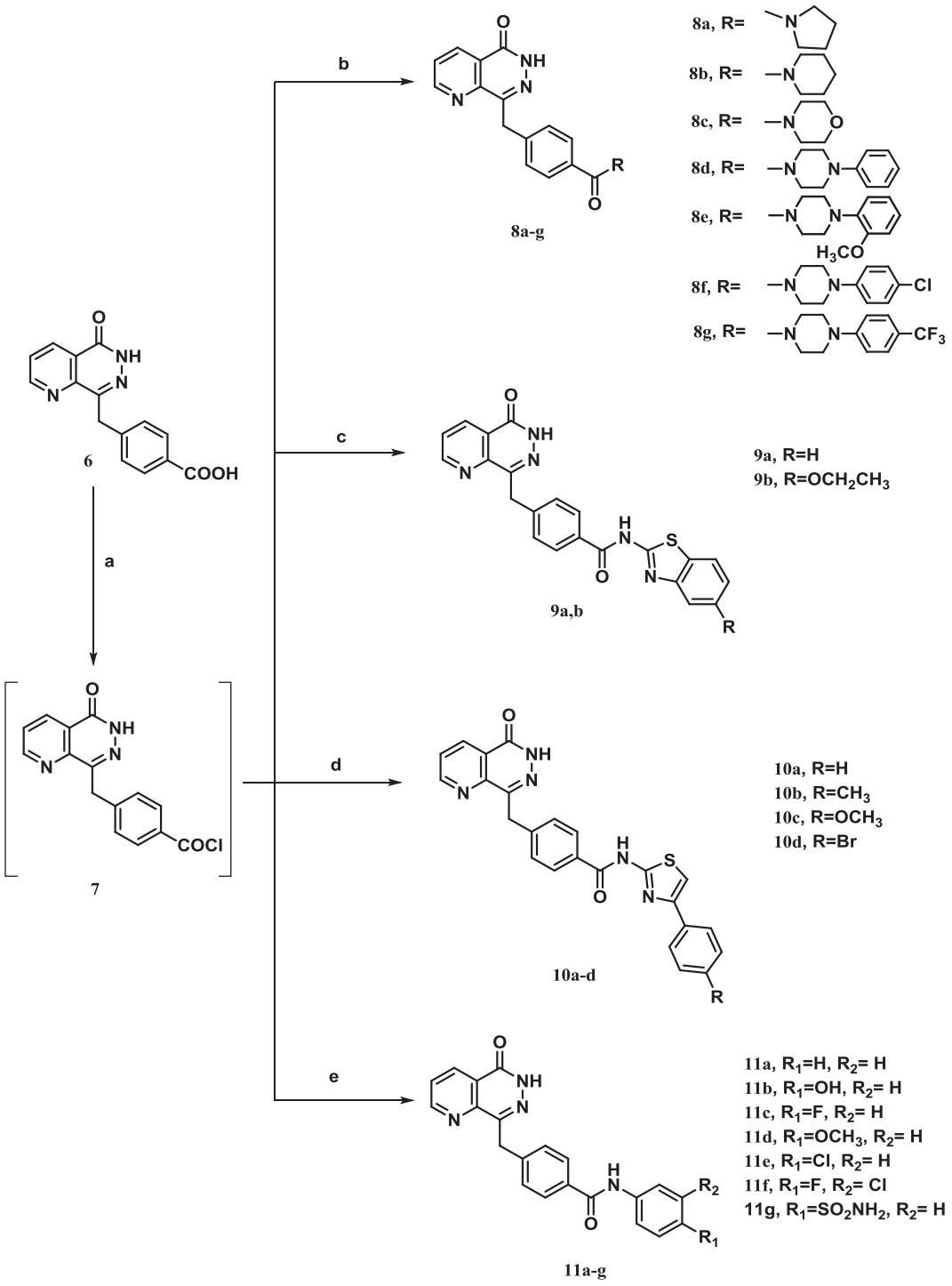

Reagents and solvents: a) $SOCl_2$, b) appropriate secondry amine, TEA, DMF, c) appropriate 2-amino benzothiazole, TEA, DMF, d) substituted 2-amino phenylthiazole, TEA, DMF, e) appropriate aniline or sulfanilamide, TEA, DMF.

Scheme 2. Synthesis of the designed compounds **8a-e, 9a and b, 10a-d** and **11a-g**.

Moreover, a specific π-stacking interaction for the designed PARP inhibitors was observed between the pyridazinone ring and the phenyl moiety of Tyr907. These interactions are also displayed in the binding of Olaparib to the PARP-1 active site which suggested the potential activity of the novel compounds. The docking results of the most active compounds and Olaparib with amino acids of the active site are summarized in Table 2. The highest inhibition of PARP-1 detected for compounds **8a**, **10a**, **8e**, **10c**, **11d** and **11g** suggested a detailed analysis of their possible binding modes in the catalytic domain of PARP-1. The pyridopyridazinones **8a** and **8e** showed slightly lower binding energy score compared to Olaparib while compounds **10a** (Fig. 6), **10c**, **11d** and **11g** displayed comparable or even higher binding to PARP-1. Both Ser904 and Gly863 were engaged in main hydrogen bond interactions with the carboxamide group of the target derivative **8a**. The pyridazinone ring of **8a** showed clear π-stack interaction with Tyr-907. Additionally, **8a** was involved in hydrogen-π interactions with Tyr896

Table 1
In vitro inhibitory activity of the synthesized compounds against PARP-1.

Compound	IC_{50} (nM)	pIC_{50} ± S.D
8a	36.74	7.43 ± 0.02
8b	133.03	6.87 ± 0.015
8c	165.08	6.78 ± 0.015
8d	71.58	7.15 ± 0.015
8e	48.90	7.31 ± 0.015
8f	180.92	6.74 ± 0.015
8g	142.001	6.85 ± 0.02
9a	63.81	7.20 ± 0.015
9b	69.79	7.16 ± 0.015
10a	45.52	7.34 ± 0.02
10b	218.78	6.66 ± 0.02
10c	53.83	7.27 ± 0.02
10d	60.87	7.22 ± 0.015
11a	634.88	6.20 ± 0.015
11b	64.33	7.19 ± 0.02
11c	283.85	6.55 ± 0.015
11d	54.18	7.27 ± 0.015
11e	269.19	6.57 ± 0.02
11f	82.94	7.08 ± 0.02
11g	56.46	7.25 ± 0.02
Olaparib	34.15	7.47 ± 0.015

and Lys903 in a similar manner to Olaparib. It is worth to mention that the key hydrogen bonds displayed by **8a** characteristic of this class of inhibitors were nearly of the same length of that of Olaparib or even shorter and this may in part account for its high biological activity despite the lower binding energy. The methoxy group attached to the piperazine moiety of **8e** showed additional hydrogen-π interaction with Arg878. Compounds **8e** and **10a** were stabilized through three hydrogen–π interactions with Tyr896 and Arg878. Compound **10c** was involved in a new hydrogen-π interaction with Pro881. Moreover, compound **11d** formed an additional hydrogen bond to Arg878, similar to that of Olaparib via the oxygen of methoxy group, in addition to a characteristic hydrogen-π interaction with the same amino acid. Finally, the pyridopyridazinone **11g** achieved two hydrogen bonds with Arg878 via its sulphone moiety. These findings revealed a good correlation between the molecular modeling studies and the biological results.

3.2. Drug-likeness properties

The drug-likeness profiles for Olaparib **II** and the target compounds **8a** and **8e** were predicted using SwissADME server [30]. The results of the Swiss ADME prediction of drug likeness of these compounds are shown in Supplementary Table 1. Compounds **8a** and **8e** showed no violation to Lipinski and other pharmacokinetics filters, and contained no alerts for Pan Assay Interfering Substances (PAINS). Furthermore, the pyridopyridazinones **8a** and **8e** exhibited a predicted consensus log Po/w value of 2.41 and 2.92, respectively with good to moderate water solubility, high GIT absorption and no BBB permeability which correlated with minimal predicted CNS adverse effects. Moreover, the oral bioavailability radar chart of compound **8a** and **8e** indicated their good predicted oral bioavailability and promising pharmacokinetic properties (For details see Supplementary Figs. 1 and 2).

4. Conclusion

This research work aimed at discovering novel PARP-1 inhibitors with a significant advantage of prospective improved physicochemical properties and where a wide variety of substituents can be tolerated. The design of the target compounds was based on the Olaparib template model which was modified through replacement of its phthalazine ring with an isosteric pyridopyridazine nucleus and through appending of various chemical fragments to its benzyl side chain. Most compounds possessed inhibitory potencies comparable to, or slightly lower than Olaparib. Molecular docking study was performed prior to synthesis to assess the design of the new compounds and after biological testing to have a deep insight of the SAR of the compounds. Drug likeness of the compounds was also predicted *in silico* and revealed promising pharmacokinetic properties of the newly synthesized compounds. Therefore, this study represents an introduction of a new ring system (pyridopyridazinone) in the field of NAD-like PARP-1 inhibitors. As a preliminary study, a success was achieved in presenting compounds with activity in the nanomolar level. We thus believe that these compounds represent good hits for further study of structure–activity relationship and optimization.

5. Experimental

5.1. Chemistry

5.1.1. General

Starting materials and solvents were purchased from commercial suppliers and were used without further purification. NMR and Infrared spectra were performed at the Microanalytical Unit-Faculty of Pharmacy, Cairo University. ^{1}HNMR spectra were recorded on a Bruker Ascend 400 MHz spectrometer and ^{13}C spectra were run at 100 MHz in deuterated dimethylsulfoxide (DMSO-*d*6). Chemical shift values (δ) are given in parts per million (ppm). Coupling constants are given in hertz (Hz) and spin multiplicities are given as s (singlet), d (doublet), dd (doublet of doublet), t (triplet), q (quartet) or m (multiplet). Infrared spectra (IR) were recorded as potassium bromide discs on Schimadzu FT-IR 8400S spectrophotometer (Kyoto, Japan) and expressed in wave number (υ_{max}, cm^{-1}). TLC was performed using silica gel/TLC cards DC-Alufolien-Kiesel gel (Vilber GmbH, Germany) with fluorescent indicator UV254 using chloroform: methanol 8.5: 1.5 as the eluting system and the spots were visualized using Vilber Lourmet ultraviolet lamp (Vilber GmbH, Germany) at = 254 nm. Melting points were determined by open capillary tube method using Electrothermal 9100 melting point apparatus (Staffordshire, UK) and are uncorrected. Mass spectral data are given as *m/z* (relative abundance %). Elemental analyses were carried out at the Regional Center for Mycology and Biotechnology, Al-Azhar University, Egypt. Compounds **2**, **3** [28,29] and **4** [31,32] were synthesized as reported in the literature.

5.1.2. 4-(5-Hydroxy-7-oxo-7H-cyclopenta[b]pyridin-6-yl)benzoic acid *5*

A cold solution of CH_3ONa (0.8 g, 35 mmol) in MeOH (24 mL) was added dropwise to a mixture of compound **4** (1 g, 7.4 mmol) and 4-carboxybenzaldehyde (1.**12** g, 8 mmol) in ethyl acetate (8 mL). The reaction mixture was stirred at room temperature for 1 h, heated to reflux for 1 h, then the solvent was distilled off under reduced pressure. The residue was poured into ice water, acidified with glacial acetic acid to pH 2–3 and separated by filtration to give compound **5**. Yield: 65%, m.p.: > 300 °C, I.R. (KBr, cm^{-1}): υ_{max} 3537 (OH), 3097 (CH aromatic), 2638–2515 (carboxylic OH), 1678 (C═O), 1600 (C═N), 1535 (C═C), ^{1}H NMR: δ 7.19–7.22 (m, 1H, pyridyl-H), 7.48 (dd, 1H, *J* = 1.4, 7.1 Hz, pyridyl-H), 7.75 (d, 2H, *J* = 8.7 Hz, phenyl-H), 8.37 (dd, 1H, *J* = 1.4, 5.1 Hz, pyridyl-H), 8.62 (d, 2H, *J* = 8.7 Hz, phenyl-H), 12.26 (s, 2H, 2 OH exchanged by D_2O). Anal. Calcd. for $C_{15}H_9NO_4$ (267.24): C, 67.42; H, 3.39; N, 5.24. Found: C, 67.14; H, 3.62; N, 5.49.

5.1.3. 4-((5-Oxo-5,6-dihydropyrido[2,3-d]pyridazin-8-yl)methyl)benzoic acid *6*

A solution of 99% hydrazine hydrate (3 mL, 94 mmol) and compound **5** (1 g, 3.75 mmol) was stirred at 100 °C for 5 h. The reaction mixture was allowed to cool and the separated product was filtered off, washed with ethanol and left to dry. The obtained solid was dissolved in distilled water and the solution was acidified with acetic acid. The resulting precipitate was filtered off, washed with water and dried to give compound **6** which was recrystallized from DMF. Yield: 40%, m.p.:

Table 2
Docking scores as "S" (Kcal mol^{-1}) and bond interactions of the most active derivatives with key amino acids of PARP-1.

Cpd. No.	S (Kcal mol^{-1})	No. of bonds	Distance (A°)	Amino acids involved	Interacting groups
8a	−29.08	6	2.87	Gly863	H-bond with NH of pyridazinone
			2.99	Gly863	H-bond with C═O of pyridazinone
			2.77	Ser904	H-bond with C═O of pyridazinone
				Tyr907	π-π stack with pyridazinone ring
				Tyr896	H-π interaction with pyridyl ring
				Lys903	H-π interaction with pyridyl ring
8e	−29.32	7	3.14	Gly863	H-bond with NH of pyridazinone
			2.92	Gly863	H-bond with C═O of pyridazinone
			3.25	Ser904	H-bond with C═O of pyridazinone
				Tyr907	π-π stack with pyridazinone ring
				Tyr896	H-π interaction with pyridyl ring
				Tyr896	H-π interaction with phenyl ring
				Arg878	H-π interaction with methoxyphenyl
10a	−35.05	7	2.85	Gly863	H-bond with NH of pyridazinone
			3.17	Gly863	H-bond with C═O of pyridazinone
			2.95	Ser904	H-bond with C═O of pyridazinone
				Tyr907	π-π stack with pyridazinone ring
				Tyr896	H-π interaction with pyridyl ring
				Tyr896	H-π interaction with phenyl ring
				Arg878	H-π interaction with thiazole ring
10c	−32.39	6	2.91	Gly863	H-bond with NH of pyridazinone
			2.95	Gly863	H-bond with C═O of pyridazinone
			2.99	Ser904	H-bond with C═O of pyridazinone
				Tyr907	π-π stack with pyridazinone ring
				Tyr896	H-π interaction with pyridyl ring
				Pro881	H-π interaction with methoxy phenyl ring
11d	−32.35	7	2.90	Gly863	H-bond with NH of pyridazinone
			2.97	Gly863	H-bond with C═O of pyridazinone
			3.17	Ser904	H-bond with C═O of pyridazinone
				Tyr907	π-π stack with pyridazinone ring
				Tyr896	H-π interaction with pyridyl ring
			3.00	Arg878	H-bond with O of methoxy
				Arg878	H-π interaction with methoxy phenyl
11g	−31.19	7	2.98	Gly863	H-bond with NH of pyridazinone
			2.93	Gly863	H-bond with C═O of pyridazinone
			3.04	Ser904	H-bond with C═O of pyridazinone
				Tyr907	π-π interaction with pyridazinone ring
				Tyr896	H-π interaction with pyridyl ring
			2.93	Arg878	H-bond with O of sulfone
			3.19	Arg878	H-bond with amino of sulfone
Olaparib	−31.95	8	2.81	Gly863	H-bond with NH of pyridazinone
			2.92	Gly863	H-bond with C═O of pyridazinone
			2.77	Ser904	H-bond with C═O of pyridazinone
				Tyr907	π-π stack with pyridazinone ring
			2.83	Tyr896	H-bond with C═O linker
				Tyr896	H-π interaction with phenyl of phthalazinone
				Lys903	H-π interaction with phenyl of phthalazinone
			2.89	Arg878	H-bond with C═O linker

230–231 °C, I.R (KBr, cm^{-1}): υ_{max} 3244 (NH), 3086 (CH aromatic), 2931 (CH aliphatic), 2931–2854 (carboxylic OH), 1701 (2C═O), 1593 (C═N), 1550 (C═C), ^{1}H NMR: δ 4.40 (s, 2H, CH_2), 7.43 (d, 2H, J = 8.1 Hz, phenyl-H), 7.83–7.87 (m, 3H, pyridyl-H and phenyl-H), 8.35 (d, 1H, J = 8.24 Hz, pyridyl-H), 9.04 (d, 1H, J = 4.3 Hz, pyridyl-H), 12.50 (s, 1H, carboxylic OH exchanged by D_2O), 12.84 (s, 1H, NH exchanged by D_2O). ^{13}C NMR: δ 37.5 (CH_2 carbon), 126.9, 128.4, 129.4, 129.6, 130.1, 134.6, 143.5, 144.2, 144.9 (Ar-Cs), 154.1 (C═N), 159.1 (C═O), 167.6 (C═O). Anal. Calcd. for $C_{15}H_{11}N_3O_3$ (281.27): C, 64.05; H, 3.94; N, 14.94. Found: C, 63.89; H, 4.09; N, 15.21.

*5.1.4. 4-((5-Oxo-5,6-dihydropyrido[2,3-d]pyridazin-8-yl)methyl)benzoyl chloride **7***

Compound **6** (0.5 g, 1.8 mmol) was heated under reflux with thionyl chloride (5 mL) and DMF (3 drops) for 2 h., excess thionyl chloride was distilled off under reduced pressure and residual thionyl chloride was removed azeotropically with dry benzene. The acid chloride thus obtained was used for further reactions without purification.

*5.1.5. General procedure for the synthesis of compounds **8a-g, 9a and b, 10a-d and 11a-g***

The crude acid chloride **7** obtained in the previous step was cooled to 0 °C and dissolved in dry DMF (2 mL). To this solution, the appropriate amine (1.65 mmol) and triethylamine (1 mL, 10 mmol) were added. The reaction mixture was stirred at 100 °C for 6 h. The solution was poured over crushed ice and the precipitated solid was filtered off, washed with water, dried and recrystallized from the suitable solvent.

*5.1.5.1. **8-(4-(Pyrrolidine-1-carbonyl)benzyl)pyrido[2,3-d]pyridazin-5(6H)-one 8a**.* Yield: 60%, m.p.: 185–187 °C, I.R (KBr, cm^{-1}): υ_{max} 3425 (NH), 3159 (CH aromatic), 2970 (CH aliphatic), 1690, 1654 (2C═O), 1612 (C═N), 1562 (C═C), ^{1}H NMR: δ 1.75–1.85 (m, 4H, pyrrolidinyl-H), 3.33 (t, 4H, pyrrolidinyl-H, J = 6.28 Hz), 4.36 (s, 2H, CH_2), 7.34 (d, 2H, J = 8.0 Hz, phenyl-H), 7.44 (d, 2H, J = 8.2 Hz, phenyl-H), 7.82–7.88 (m, 1H, pyridyl-H), 8.37 (dd, 1H, J = 1.2, 8.2 Hz, pyridyl-H), 9.04 (dd, 1H, J = 1.2, 4.4 Hz, pyridyl-H), 12.86 (s, 1H, NH exchanged by D_2O). ^{13}C NMR: δ 24.3, (pyrrolidine-Cs), 37.4 (CH_2 carbon), 45.8 (pyrrolidine-Cs),

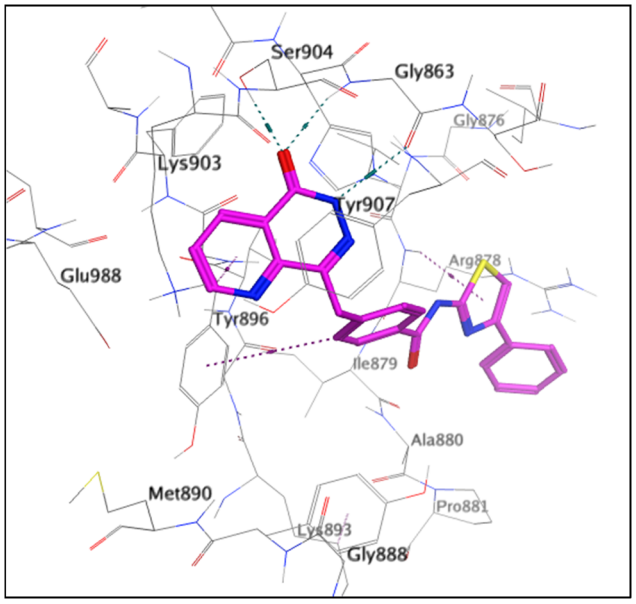

Fig. 6. 3D diagram of compound **10a** showing its interaction with the PARP-1 active site.

127.7, 128.3, 128.9, 134.6, 135.9, 139.9, 144.3, 145.1, 154.1 (Ar-Cs), 159.0 (C═N), 161.1 (C═O), 168.4 (C═O). Anal. Calcd. for $C_{19}H_{18}N_4O_2$ (334.38): C, 68.25; H, 5.43; N, 16.76. Found: C, 68.47; H, 5.66; N, 16.91.

5.1.5.2. 8-(4-(Piperidine-1-carbonyl)benzyl)pyrido[2,3-d]pyridazin-5(6H)-one ***8b***. Yield: 71%, m.p.: 168–170 °C, I.R (KBr, cm^{-1}): υ_{max} 3444 (NH), 3124 (CH aromatic), 2931(CH aliphatic), 1680, 1670 (2C═O), 1620 (C═N), 1504 (C═C), ^{1}H NMR: δ 1.48–1.74 (m, 10*H*, piperidinyl-H), 4.36 (s, 2H, CH_2), 7.28 (d, 2H, J = 8.04 Hz, phenyl-H), 7.37 (d, 2H, J = 8.2 Hz, phenyl-H), 7.85–7.88 (m, 1H, pyridyl-H), 8.4 (d, 1H, J = 1.2, 7.92 Hz, pyridyl-H), 9.05 (d, 1H, J = 3.2 Hz, pyridyl-H), 12.79 (s, 1H, NH exchanged by D_2O). ^{13}C NMR: δ 24.5, 26.4 (piperidine-Cs), 37.4 (CH_2 carbon), 50.1 (piperidine-Cs), 126.3, 127.4, 128.2, 129.1, 131.3, 134.6, 135.1, 139.7, 145.1 (Ar-Cs), 154.0 (C═N), 159.0 (C═O), 169.2 (C═O). MS *m/z* (%): 348 (M^+, 21.36%), 84 (100%). Anal. Calcd. for $C_{20}H_{20}N_4O_2$ (348.41): C, 68.95; H, 5.79; N, 16.08. Found: C, 69.23; H, 5.87; N, 16.24.

5.1.5.3. 8-(4-(Morpholine-4-carbonyl)benzyl)pyrido[2,3-d]pyridazin-5(6H)-one ***8c***. Yield: 45%, m.p.: 180–182 °C, I.R (KBr, cm^{-1}): υ_{max} 3464 (NH), 3100(CH aromatic), 2920 (CH aliphatic), 1666 (2C═O), 1620 (C═N), 1543 (C═C), ^{1}H NMR: δ 3.41 (t, 2H, J = 5.00 Hz, morpholinyl-H), 3.59 (t, 2H, J = 5.12 Hz, morpholinyl -H), 3.67 (t, 2H, J = 4.56 Hz, morpholinyl -H), 3.72 (t, 2H, J = 3.88 Hz, morpholinyl -H), 4.33 (s, 2H, CH_2), 7.32 (d, 2H, J = 8.0 Hz, phenyl-H), 7.37 (d, 2H, J = 8.2 Hz, phenyl-H), 7.66–7.69 (m, 1H, J = 3.8, 7.4 Hz, pyridyl-H), 8.03 (d, 1H, J = 1.2, 6.2 Hz, pyridyl-H), 9.09 (d, 1H, J = 3.3 Hz, pyridyl-H), 11.41 (s, 1H, NH exchanged by D_2O). Anal. Calcd. for $C_{19}H_{18}N_4O_3$ (350.38): C, 65.13; H, 5.18; N, 15.99. Found: C, 65.28; H, 5.34; N, 16.21.

5.1.5.4. 8-(4-(4-Phenylpiperazine-1-carbonyl)benzyl)pyrido[2,3-d] pyridazin-5(6H)-one ***8d***. Yield: 70%, m.p.: 136–138 °C, I.R (KBr, cm^{-1}): υ_{max} 3553 (NH), 3089 (CH aromatic), 2920 (CH aliphatic), 1680, 1666 (2C═O), 1620 (C═N), 1496 (C═C), ^{1}H NMR: δ 3.35 (s, 8H, piperazinyl-H), 4.37 (s, 2H, CH_2), 6.81 (d, 2H, J = 6.7 Hz, phenyl piperazine-H), 6.94 (d, 2H, J = 8.2 Hz, phenyl piperazine-H), 7.23 (t, 3H, J = 7.6 Hz, 2 phenyl-H and 1 phenyl piperazine-H), 7.39 (d, 2H, J = 5.2, phenyl -H), 7.87–7.90 (m, 1H, pyridyl-H), 8.40 (d, 1H, J = 8.1 Hz, pyridyl-H), 9.05 (d, 1H, J = 4.1 Hz, pyridyl-H), 12.86 (s, 1H, NH exchanged by D_2O). Anal. Calcd. for $C_{25}H_{23}N_5O_2$ (425.49): C, 70.57; H, 5.45; N, 16.46. Found: C, 70.39; H, 5.63; N, 16.80.

5.1.5.5. 8-(4-(4-(2-Methoxyphenyl)piperazine-1-carbonyl)benzyl)pyrido [2,3-d]pyridazin-5(6H)-one ***8e***. Yield: 65%, m.p.: 150–152 °C, I.R (KBr, cm^{-1}): υ_{max} 3444 (NH), 3062 (CH aromatic), 2924 (CH aliphatic), 1666 (2C═O), 1624 (C═N), 1500 (C═C), ^{1}H NMR: δ 2.95 (s, 8H, piperazinyl-H), 3.77 (s, 3H, methoxy-H), 4.37 (s, 2H, CH_2), 6.88–6.95 (m, 4H, methoxy phenyl-H), 7.38 (d, 4H, J = 8.84 Hz, phenyl-H), 7.87–7.90 (m, 1H, pyridyl-H), 8.40 (d, 1H, J = 8.1 Hz, pyridyl-H), 9.05 (d, 1H, J = 3.4 Hz, pyridyl-H), 12.86 (s, 1H, NH exchanged by D_2O). ^{13}C NMR: δ 37.4 (CH_2 carbon), 46.2, 50.7 (piperazine-Cs), 55.8 (OCH_3 carbon) 112.3, 118.8, 121.2, 123.4, 126.5, 127.9, 128.4, 128.8, 129.1, 134.6, 139.9, 141.1, 144.3, 145.1, 152.5 (Ar-Cs), 154.1 (C═N), 159.1 (C═O), 169.2 (C═O). Anal. Calcd. for $C_{26}H_{25}N_5O_3$ (455.52): C, 68.56; H, 5.53; N, 15.37. Found: C, 68.79; H, 5.80; N, 15.61.

5.1.5.6. 8-(4-(4-(4-Chlorophenyl)piperazine-1-carbonyl)benzyl)pyrido [2,3-d]pyridazin-5(6H)-one ***8f***. Yield: 77%, m.p.: 188–190 °C, I.R (KBr, cm^{-1}): υ_{max} 3421 (NH), 3066 (CH aromatic), 2924 (CH aliphatic), 1670 (2C═O), 1624 (C═N), 1496 (C═C), ^{1}H NMR: δ 3.14 (s, 8H, piperazinyl-H), 4.37 (s, 2H, CH_2), 6.94–6.97 (m, 2H, chloro phenyl-H), 7.23–7.27 (m, 4H, chloro phenyl and phenyl-H), 7.36–7.41 (m, 2H, phenyl-H), 7.87–7.90 (m, 1H, pyridyl-H), 8.40 (dd, 1H, J = 1.3, 8.3 Hz, pyridyl-H), 9.05 (dd, 1H, J = 1.3, 4.7 Hz, pyridyl-H), 12.85 (s, 1H, NH exchanged by D_2O). ^{13}C NMR: δ 37.3 (CH_2 carbon), 48.5, 48.7 (piperazine-Cs), 117.7, 123.3, 126.5, 127.8, 128.3, 129.1, 129.2, 134.3, 134.6, 139.9, 144.3, 145.11, 149.99 (Ar-Cs), 154.1 (C═N), 159.1 (C═O), 169.3 (C═O). MS *m/z* (%): 459 (M^+, 10.16%), 461 (M + 2, 4.14%), 67 (100%). Anal. Calcd. for $C_{25}H_{22}ClN_5O_2$ (459.93): C, 65.29; H, 4.82; N, 15.23. Found: C, 65.17; H, 4.98; N, 15.41.

5.1.5.7. 8-(4-(4-(4-(Trifluoromethyl)phenyl)piperazine-1-carbonyl) benzyl)pyrido[2,3-d]pyridazin-5(6H)-one ***8g***. Yield: 65%, m.p.: 120–122 °C, I.R (KBr, cm^{-1}): υ_{max} 3464 (NH), 3116 (CH aromatic), 2924 (CH aliphatic), 1670 (2C═O), 1635 (C═N), 1550 (C═C), ^{1}H NMR: δ 3.35 (s, 8H, piperazinyl-H), 4.37 (s, 2H, CH_2), 7.18–7.24 (m, 2H, trifluorophenyl-H), 7.37–7.45 (m, 6H, trifluorophenyl-H and phenyl-H), 7.87–7.90 (m, 1H, pyridyl-H), 8.40 (d, 1H, J = 8.2 Hz, pyridyl-H), 9.05 (d, 1H, J = 3.5 Hz, pyridyl-H), 12.86 (s, 1H, NH exchanged by D_2O). Anal. Calcd. for $C_{26}H_{22}F_3N_5O_2$ (493.49): C, 63.28; H, 4.49; N, 14.19. Found: C, 63.56; H, 4.65; N, 14.53.

5.1.5.8. N-(Benzo[d]thiazol-2-yl)-4-((5-oxo-5,6-dihydropyrido[2,3-d] pyridazin-8-yl)methyl)benzamide ***9a***. Yield: 70%, m.p.: 200–202 °C, I.R (KBr, cm^{-1}): υ_{max} 3421 (2NH), 3066 (CH aromatic), 2978 (CH aliphatic), 1666 (2C═O), 1593 (C═N), 1531(C═C), ^{1}H NMR: δ 4.42 (s, 2H, CH_2), 7.49 (d, 2H, J = 8.0 Hz, phenyl-H), 7.80 (d, 2H, J = 8.6 Hz, phenyl-H), 7.87–7.92 (m, 2H, 1 benzothiazolyl-H and 1 pyridyl-H), 8.04 (t, 2H, J = 7.0 Hz, benzothiazolyl -H), 8.38 (t, 1H, J = 8.4 Hz, benzothiazolyl -H), 8.66 (s, 1H, pyridyl-H), 9.05 (d, 1H, J = 4.0 Hz, pyridyl-H), 10.45 (s, 1H, NH exchanged by D_2O), 12.86 (s, 1H, NH exchanged by D_2O). ^{13}C NMR: δ 37.3 (CH_2 carbon), 112.3, 113.2, 120.3, 123.2, 126.4, 128.3, 128.5, 129.2, 133.6, 134.5, 134.6, 144.3, 145.1, 149.8, 154.1, 155.4, 159.1 (Ar-Cs), 160.3 (C═O), 166.0 (C═O). Anal. Calcd. for $C_{22}H_{15}N_5O_2S$ (413.45): C, 63.91; H, 3.66; N, 16.94. Found: C, 63.75; H, 3.89; N, 17.21.

5.1.5.9. N-(6-Ethoxybenzo[d]thiazol-2-yl)-4-((5-oxo-5,6-dihydropyrido [2,3-d]pyridazin-8-yl)methyl)benzamide ***9b***. Yield: 65%, m.p.: 185–187 °C, I.R (KBr, cm^{-1}): υ_{max} 3421 (2NH), 3066 (CH aromatic), 2924 (CH aliphatic), 1670 (2C═O), 1604 (C═N), 1550 (C═C), ^{1}H NMR: δ 1.34 (t, 3H, J = 8.0 Hz, CH_3CH_2), 4.06 (q, 2H, J = 6.9 Hz, CH_3CH_2), 4.42 (s, 2H, CH_2), 6.90 (dd, 1H, J = 2.4, 8.8 Hz, benzothiazolyl -H), 7.27–7.56 (m, 3H, 2 benzothiazolyl-H and 1 pyridyl-H), 7.64 (d, 2H, J = 8.8 Hz, phenyl -H), 7.86 (d, 2H,

J = 7.8 Hz, phenyl -H), 8.54 (s, 1H, pyridyl-H), 9.04 (d, 1H, J = 4.8 Hz, pyridyl-H), 12.86 (s, 2H, NH exchanged by D_2O). MS *m/z* (%): 457 (M^+, 64.98%), 64 (100%). Anal. Calcd. for $C_{24}H_{19}N_5O_3S$ (457.51): C, 63.01; H, 4.19; N, 15.31. Found: C, 63.29; H, 4.37; N, 15.48.

5.1.5.10. 4-((5-Oxo-5,6-dihydropyrido[2,3-d]pyridazin-8-yl)methyl)-N-(4-phenylthiazol-2-yl)benzamide ***10a***. Yield: 66%, m.p.: 199–201 °C, I.R (KBr, cm^{-1}): υ_{max} 3421 (2NH), 3124 (CH aromatic), 2924 (CH aliphatic), 1732, 1681 (2C═O), 1620 (C═N), 1543 (C═C), ^{1}H NMR: δ 4.40 (s, 2H, CH_2), 7.34–7.42 (m, 5H, phenyl-H), 7.44 (s, 1H, thiazolyl -H), 7.78–7.88 (m, 5H, 4 phenyl-H and 1 pyridyl-H), 8.32 (s, 1H, J = 7.96 Hz, pyridyl-H), 9.04 (d, 1H, J = 4.3 Hz, pyridyl-H), 12.85 (s, 2H, NH exchanged by D_2O). MS *m/z* (%): 439 (M^+, 22.44%), 43 (100%). Anal. Calcd. for $C_{24}H_{17}N_5O_2S$ (439.49): C, 65.59; H, 3.90; N, 15.94. Found: C, 65.83; H, 4.12; N, 15.78.

5.1.5.11. 4-((5-Oxo-5,6-dihydropyrido[2,3-d]pyridazin-8-yl)methyl)-N-(4-(p-tolyl)thiazol-2-yl)benzamide ***10b***. Yield: 50%, m.p.: 160–162 °C, I.R (KBr, cm^{-1}): υ_{max} 3421 (2NH), 3024 (CH aromatic), 2924 (CH aliphatic), 1732, 1666 (2C═O), 1612 (C═N), 1465 (C═C), ^{1}H NMR: δ 2.50 (s, 3H, CH_3), 4.39 (s, 2H, CH_2), 7.16 (d, 4H, J = 8.12 Hz, methylphenyl-H), 7.34 (s, 1H, thiazolyl -H), 7.66 (d, 1H, J = 7.8 Hz, pyridyl-H), 7.77 (d, 4H, J = 7.9 Hz, phenyl-H), 8.36 (s, 1H, pyridyl-H), 9.04 (s, 1H, pyridyl-H), 12.86 (s, 2H, NH exchanged by D_2O). Anal. Calcd. for $C_{25}H_{19}N_5O_2S$ (453.13): C, 66.21; H, 4.22; N, 15.44. Found: C, 66.48; H, 4.39; N, 15.61.

5.1.5.12. N-(4-(4-Methoxyphenyl)thiazol-2-yl)-4-((5-oxo-5,6-dihydropyrido[2,3-d]pyridazin-8-yl)methyl)benzamide ***10c***. Yield: 52%, m.p.: 145–147 °C, I.R (KBr, cm^{-1}): υ_{max} 3444 (2NH), 3116 (CH aromatic), 2999 (CH aliphatic), 1670 (2C═O), 1620 (C═N), 1485 (C═C), ^{1}H NMR: δ 3.78 (s, 3H, OCH_3), 4.43 (s, 2H, CH_2), 6.90 (d, 2H, J = 8.8 Hz, methoxyphenyl-H), 7.00 (d, 2H, J = 8.4 Hz, methoxyphenyl-H), 7.25 (s, 1H, thiazolyl-H), 7.81 (d, 2H, J = 8.4 Hz, phenyl-H), 7.88 (d, 2H, J = 8.3 Hz, phenyl-H), 8.07 (d, 1H, J = 8.0 Hz, pyridyl-H), 8.39 (d, 1H, J = 4.0 Hz, pyridyl-H), 9.05 (d, 1H, J = 4.1 Hz, pyridyl-H), 12.86 (s, 2H, NH exchanged by D_2O). Anal. Calcd. for $C_{25}H_{19}N_5O_3S$ (469.52): C, 63.95; H, 4.08; N, 14.92. Found: C, 64.23; H, 4.21; N, 15.13.

5.1.5.13. N-(4-(4-Bromophenyl)thiazol-2-yl)-4-((5-oxo-5,6-dihydropyrido[2,3-d]pyridazin-8-yl)methyl)benzamide ***10d***. Yield: 55%, m.p.: 142–144 °C, I.R (KBr, cm^{-1}): υ_{max} 3417, 3425 (2NH), 3116 (CH aromatic), 2920 (CH aliphatic), 1666 (2C═O), 1620 (C═N), 1469 (C═C), ^{1}H NMR: δ 4.42 (s, 2H, CH_2), 7.08 (s, 1H, thiazolyl-H), 7.50–7.59 (m, 5H, 4 bromophenyl-H and 1 pyridyl-H), 7.74 (d, 2H, J = 8.3 Hz, phenyl-H), 7.84 (d, 2H, J = 8.2 Hz, phenyl-H), 8.37 (s, 1H, pyridyl-H), 9.04 (s, 1H, pyridyl-H), 12.88 (s, 2H, NH exchanged by D_2O). ^{13}C NMR: δ 37.5 (CH_2 carbon), 127.9, 128.2, 128.9, 129.4, 129.6, 131.4, 131.8, 132.1, 134.5, 137.9, 144.0, 146.9, 150.1, 151.2, 153.9, 157.5, 159.3, (Ar-Cs), 162.4 (C═O), 163.3 (C═O). Anal. Calcd. for $C_{24}H_{16}BrN_5O_2S$ (518.39): C, 55.61; H, 3.11; N, 13.51. Found: C, 55.89; H, 3.27; N, 13.74.

5.1.5.14. 4-((5-Oxo-5,6-dihydropyrido[2,3-d]pyridazin-8-yl)methyl)-N-phenylbenzamide ***11a***. Yield: 50%, m.p.: 205–207 °C, I.R (KBr, cm^{-1}): υ_{max} 3417 (2NH), 3055 (CH aromatic), 2924 (CH aliphatic), 1666 (2C═O), 1597 (C═N), 1539 (C═C), ^{1}H NMR: δ 4.40 (s, 2H, CH_2), 7.07–7.09 (m, 3H, aniline-H), 7.32 (d, 2H, J = 7.1 Hz, aniline-H), 7.47 (d, 2H, J = 7.4 Hz, phenyl-H), 7.75 (d, 2H, *Jm* = 8.0 Hz, phenyl-H), 7.88 (d, 2H, J = 7.5 Hz, pyridyl-H), 9.02 (d, 1H, J = 9.0 Hz, pyridyl-H), 10.19 (s, 1H, NH exchanged by D_2O), 12.88 (s, 1H, NH exchanged by D_2O). Anal. Calcd. for $C_{21}H_{16}N_4O_2$ (356.38): C, 70.77; H, 4.53; N, 15.72. Found: C, 70.89; H, 4.67; N, 15.89.

5.1.5.15. N-(4-Hydroxyphenyl)-4-((5-oxo-5,6-dihydropyrido[2,3-d]pyridazin-8-yl)methyl)benzamide ***11b***. Yield: 77%, m.p.: 239–241 °C, I.R (KBr, cm^{-1}): υ_{max} 3433 (2NH), 3267 (OH), 3070 (CH aromatic), 2935 (CH aliphatic), 1666 (2C═O), 1608 (C═N), 1512 (C═C), ^{1}H NMR: δ 4.42 (s, 2H, CH_2), 7.23 (d, 1H, J = 8.6 Hz, hydroxy phenyl-H), 7.43–7.55 (m, 3H, hydroxy phenyl-H), 7.81 (d, 2H, J = 8.7 Hz, phenyl-H), 7.83–7.89 (m, 2H, phenyl-H), 8.06 (d, 1H, J = 7.8 Hz, pyridyl-H), 8.37 (d, 1H, J = 7.9 Hz, pyridyl-H), 9.05 (s, 1H, pyridyl-H), 9.24 (s, 1H, OH exchanged by D_2O), 10.29 (s, 1H, NH exchanged by D_2O), 12.86 (s, 1H, NH mexchanged by D_2O). ^{13}C NMR: δ 37.4 (CH_2 carbon), 115.4, 122.3, 122.4, 126.4, 128.3, 128.7, 129.3, 129.8, 130.6, 134.8, 141.3, 143.6, 145.8 (Ar-Cs), 154.3 (C═N), 159.5 (C═O), 166.4 (C═O). Anal. Calcd. for $C_{21}H_{16}N_4O_3$ (372.38): C, 67.73; H, 4.33; N, 15.05. Found: C, 68.01; H, 4.50; N, 15.32.

5.1.5.16. N-(4-Fluorophenyl)-4-((5-oxo-5,6-dihydropyrido[2,3-d]pyridazin-8-yl)methyl)benzamide ***11c***. Yield: 70%, m.p.: 263–265 °C, I.R (KBr, cm^{-1}): υ_{max} 3425, 3313 (2NH), 3070 (CH aromatic), 2927 (CH aliphatic), 1701 (2C═O), 1612 (C═N), 1527 (C═C), ^{1}H NMR: δ 4.42 (s, 2H, CH_2), 7.18 (t, 2H, J = 8.7 Hz, fluoro phenyl-H), 7.47 (d, 2H, J = 7.9 Hz, fluoro phenyl-H), 7.75–7.78 (m, 3H, 1 pyridyl-H and 2 phenyl-H), 7.87 (d, 2H, J = 8.9 Hz, phenyl-H), 8.37 (d, 1H, J = 8.0 Hz, pyridyl-H), 9.04 (d, 1H, J = 3.7 Hz, pyridyl-H), 10.24 (s, 1H, NH exchanged by D_2O), 12.87 (s, 1H, NH exchanged by D_2O). ^{13}C NMR: δ 37.5 (CH_2 carbon), 115.5, 115.7, 122.5, 122.6, 126.4, 128.3, 128.4, 129.2, 133.6, 134.6, 142.1, 144.3, 145.0 (Ar-Cs), 154.1 (C═N), 159.1 (C═O), 165.7 (C═O). Anal. Calcd. for $C_{21}H_{15}FN_4O_2$ (374.38): C, 67.37; H, 4.04; N, 14.97. Found: C, 67.55; H, 4.21; N, 15.13.

5.1.5.17. N-(4-Methoxyphenyl)-4-((5-oxo-5,6-dihydropyrido[2,3-d]pyridazin-8-yl)methyl)benzamide ***11d***. Yield: 72%, m.p.: 248–250 °C, I.R (KBr, cm^{-1}): υ_{max} 3464, 3047 (2NH), 3055 (CH aromatic), 2931 (CH aliphatic), 1700 (2C═O), 1600 (C═N), 1512 (C═C), ^{1}H NMR: δ 3.74 (s, 3H, OCH_3), 4.41 (s, 2H, CH_2), 6.91 (d, 2H, J = 8.8 Hz, methoxy phenyl-H), 7.45 (d, 2H, J = 8.0 Hz, methoxy phenyl-H), 7.64 (d, 2H, J = 8.8 Hz, phenyl-H), 7.87 (d, 3H, J = 8.0 Hz, phenyl-H and pyridyl-H), 8.37 (d, 1H, J = 8.1 Hz, pyridyl-H), 9.04 (d, 1H, J = 3.9 Hz, pyridyl-H), 10.06 (s, 1H, NH exchanged by D_2O), 12.86 (s, 1H, NH exchanged by D_2O). Anal. Calcd. for $C_{22}H_{18}N_4O_3$ (386.41): C, 68.38; H, 4.70; N, 14.50. Found: C, 68.54; H, 4.59; N, 14.67.

5.1.5.18. N-(4-Chlorophenyl)-4-((5-oxo-5,6-dihydropyrido[2,3-d]pyridazin-8-yl)methyl)benzamide ***11e***. Yield: 73%, m.p.: 253–255 °C, I.R (KBr, cm^{-1}): υ_{max} 3475, 3417 (2NH), 3055 (CH aromatic), 2927 (CH aliphatic), 1671 (2C═O), 1593 (C═N), 1527 (C═C), ^{1}H NMR: δ 4.42 (s, 2H, CH_2), 7.40 (d, 2H, J = 8.8 Hz, chloro phenyl-H), 7.47 (d, 2H, J = 8.0 Hz, chloro phenyl-H), 7.79 (d, 2H, J = 8.8 Hz, phenyl-H), 7.87 (d, 3H, J = 8.0 Hz, phenyl-H and pyridyl-H), 8.37 (d, 1H, J = 7.9 Hz, pyridyl-H), 9.04 (d, 1H, J = 3.7 Hz, pyridyl-H), 10.30 (s, 1H, NH exchanged by D_2O), 12.86 (s, 1H, NH exchanged by D_2O). ^{13}C NMR: δ 37.5 (CH_2 carbon), 122.2, 126.4, 127.6, 128.2, 128.3, 128.5, 128.9, 129.2, 133.5, 134.6, 138.6, 142.3, 145.0 (Ar-Cs), 154.1 (C═N), 159.1 (C═O), 165.9 (C═O). Anal. Calcd. for $C_{21}H_{15}ClN_4O_2$ (390.83): C, 64.54; H, 3.87; N, 14.34. Found: C, 64.77; H, 4.08; N, 14.18.

5.1.5.19. N-(3-Chloro-4-fluorophenyl)-4-((5-oxo-5,6-dihydropyrido[2,3-d]pyridazin-8-yl)methyl)benzamide ***11f***. Yield: 79%, m.p.: 210–212 °C, I.R (KBr, cm^{-1}): υ_{max} 3421 (2NH), 3066 (CH aromatic), 2927 (CH aliphatic), 1670 (2C═O), 1600 (C═N), 1500 (C═C), ^{1}H NMR: δ 4.42 (s, 2H, CH_2), 7.41 (t, 1H, J = 9.1 Hz, chloro-fluoro phenyl-H), 7.48 (d, 2H, J = 8.2 Hz, chloro-fluoro phenyl-H), 7.69–7.71 (m, 2H, phenyl-H), 7.87 (d, 3H, J = 8.3 Hz, phenyl-H and pyridyl-H), 7.97 (d, 1H, J = 5.5 Hz, pyridyl-H), 9.05 (s, 1H, pyridyl-H), 10.31 (s, 1H, NH exchanged by D_2O), 12.86 (s, 1H, NH exchanged by D_2O). Anal. Calcd. for $C_{21}H_{14}ClFN_4O_2$ (408.82): C, 61.70; H, 3.45; N, 13.70. Found: C, 61.59; H, 3.67; N, 14.02.

5.1.5.20. 4-((5-Oxo-5,6-dihydropyrido[2,3-d]pyridazin-8-yl)methyl)-N-(4-sulfamoylphenyl)benzamide ***11g***. Yield: 71%, m.p.: 151–153 °C, I.R (KBr, cm^{-1}): υ_{max} 3448, 3425 (NH_2, 2NH), 3070 (CH aromatic), 2924 (CH aliphatic), 1662 (2C═O), 1593 (C═N), 1531 (C═C), 1319, 1145 (SO_2), ^{1}H NMR: δ 4.42 (s, 2H, CH_2), 7.27 (s, 2H, NH_2 exchanged by D_2O), 7.48 (d, 2H, J = 8.1 Hz, phenyl-H), 7.74 (d, 2H, J = 8.7 Hz, phenyl-H), 7.88–7.91 (m, 5H, 4 sulfamoyl phenyl-H and 1 pyridyl-H), 8.37 (d, 1H, J = 8.2 Hz, pyridyl-H), 9.04 (d, 1H, J = 3.60 Hz, pyridyl-H), 10.47 (s, 1H, NH exchanged by D_2O), 12.87 (s, 1H, NH exchanged by D_2O). ^{13}C NMR 100 MHz: δ 35.5 (CH_2 carbon), 120.2, 127.2, 128.6, 129.2, 132.7, 134.5, 136.9, 134.6, 139.3, 141.3, 146.7, 149.8, 151.4 (Ar-Cs), 154.1 (C═N), 158.6 (C═O), 160.1 (C═O). Anal. Calcd. for $C_{21}H_{17}N_5O_4S$ (435.46): C, 57.92; H, 3.94; N, 16.08. Found: C, 58.14; H, 4.07; N, 16.32.

5.2. In vitro PARP-1 inhibitory assay

PARP-1 enzyme inhibition activity was measured for pyridopyridazinones (**8a-g**, **9a and b**, **10a-d** and **11a-g**) using a colorimetric 96-well PARP-1 assay kit (catalog no. 80580) (BPS Bioscience), according to the manufacturer's protocol. Briefly, the histone mixture was diluted 1:5 with 1x PBS, 50 µl of histone solution was added to each well and incubated at 4 °C overnight. The plate was washed three times using 200 µl PBST buffer (1x PBS containing 0.05% Tween-20) per well. Liquid was removed from the wells by tapping the strip wells on clean paper towels. To each well, 200 µl of Blocking buffer was added, followed by 60–90 min. incubation at room temperature. Then 25 µl of PARP master mixture (consisting of (2.5 µl 10x PARP buffer + 2.5 µl 10x PARP Assay mixture + 5 µl activated DNA + 15 µl distilled water) was added to each well. AZD2281 (Olaparib) was used as a positive control. 5 µl of Inhibitor solution of each well labeled as “Test Inhibitor” was added. For the “Positive Control“ and “Blank”, 5 µl of the same solution without inhibitor was added. 1x PARP buffer was prepared by adding 1 part of 10x PARP buffer to 9 parts H_2O (v/v), 20 µl of 1x PARP buffer was added to the wells designated as “Blank”. The amount of PARP-1 required for the assay was then calculated. The reaction was initiated by adding 20 µl of diluted PARP1 enzyme to the wells designated “Positive Control” and “Test Inhibitor Control”. The strip wells were incubated at room temperature for 1 h. The strip wells were then washed three times with 200 µl PBST buffer. Then, 50 µl of 50 times diluted Streptavidin-HRP with blocking buffer was added to each well, and the strips were further incubated at room temperature for 30 min. After washing the wells three times with 200 µl PBST buffer, HRP colorimetric substrate was added to each well and the plate was incubated at the room temperature until a blue color is developed in the positive control well. Then reaction was quenched with 100 mL/well of 2 M sulfuric acid, and absorbance at 450 nm was determined. Carrier solvents were assayed as negative controls. All assays were performed in triplicate. To determine the IC_{50} value for each inhibitor, the average absorbance of each inhibitor concentration was plotted against the log of the concentration of each respective inhibitor and the IC_{50} value for each plot was obtained using computer-assisted non-linear regression analyses. Data presented are the results of at least two independent experiments done in triplicate. The results of these studies are presented as mean IC_{50} (nM) and pIC_{50} ± standard deviation (SD).

5.3. In silico studies

5.3.1. Molecular docking study

Docking study of the synthesized compound was performed by Molecular Operating Environment (MOE) 2010.10 release of Chemical Computing Group, Canada [33]. The Triangle Matcher placement method and London dG scoring function were used for the evaluation of the binding pattern and binding affinity of the ligands. The X-ray crystal structure of Olaparib in complex with PARP-1 was downloaded from http://www.rscb.org/pdb (PDB ID: 5DS3) in PDB format [22]. The enzyme was prepared for docking study by removal of water molecules and ligands that are not involved in the binding. The enzyme was then prepared using Protonate 3D protocol in MOE with default options. Docking protocol was first validated by redocking of the cocrystallized ligand (Olaparib) in the active site of the receptor with energy score (S) = −31.95 kcal/mol and root mean square deviation (RMSD) of 0.396 °A. The validated docking protocol was then used to study the ligand–receptor interactions in the active site for all the designed compounds to predict their binding modes and binding affinities.

5.3.2. Drug-likeness properties

The pharmacokinetic data relevant to compound **8a** and **8e** were achieved via the free online server swissADME (http://www.swissadme.ch/index.php) where the SMILES of the compounds were inserted directly on the webpage followed by running the prediction process. A whole set of the different physical properties, pharmacokinetic parameters ADME parameters were obtained online and explained [30].

Funding

This research did not receive any specific grant from funding agencies in the public, commercial, or not-for-profit sectors.

Appendix A. Supplementary material

Supplementary data to this article can be found online at https://doi.org/10.1016/j.bioorg.2019.03.068.

References

[1] M. Hejmadi, Introduction to Cancer Biology, second ed., United Kingdom, Ventus Publishing ApS; 2010, pp. 7–10. Available from: bookboon.com.
[2] J.F. Liu, P.A. Konstantinopoulos, U.A. Matulonis, PARP inhibitors in ovarian cancer: current status and future promise, Gynecol. Oncol. 133 (2014) 362–369, https://doi.org/10.1016/j.ygyno.2014.02.039.
[3] K. Do, A.P. Chen, Molecular pathways: targeting PARP in cancer treatment, Clin. Cancer Res. 19 (2013) 977–984, https://doi.org/10.1158/1078-0432.CCR-12-0163.
[4] S.S. Kulkarni, S. Singh, J.R. Shah, W.K. Low, T.T. Talele, Synthesis and SAR optimization of quinazolin-4(3H)-ones as poly(ADP-ribose)polymerase-1 inhibitors, Eur. J. Med. Chem. 50 (2012) 264–273, https://doi.org/10.1016/j.ejmech.2012.02.001.
[5] H. Otto, P.A. Reche, F. Bazan, K. Dittmar, F. Haag, F. Koch-Nolte, In silico characterization of the family of PARP-like poly(ADP-ribosyl)transferases (pARTs), BMC Genom. 6 (2005) 139, https://doi.org/10.1186/1471-2164-6-139.
[6] M. Audebert, B. Salles, P. Calsou, Involvement of poly(ADP-ribose) polymerase-1 and XRCC1/DNA ligase III in an alternative route for DNA double-strand breaks rejoining, J. Biol. Chem. 279 (2004) 55117–55126, https://doi.org/10.1074/jbc.M404524200.
[7] V. Schreiber, F. Dantzer, J.C. Ame, G. de Murcia, Poly(ADP-ribose): novel functions for an old molecule, Nat. Rev. Mol. Cell Biol. 7 (2006) 517–528, https://doi.org/10.1038/nrm1963.
[8] N.J. Curtin, PARP inhibitors for cancer therapy, Expert Rev. Mol. Med. 7 (2005) 1–20, https://doi.org/10.1017/s146239940500904x.
[9] T.D. Penning, G.D. Zhu, V.B. Gandhi, J. Gong, X. Liu, Y. Shi, V. Klinghofer, E.F. Johnson, C.K. Donawho, D.J. Frost, V. Bontcheva-Diaz, J.J. Bouska, D.J. Osterling, A.M. Olson, K.C. Marsh, Y. Luo, V.L. Giranda, Discovery of the poly (ADP-ribose) polymerase (PARP) inhibitor 2-[(R)-2-methylpyrrolidin-2-yl]-1H-benzimidazole-4-carboxamide (ABT-888) for the treatment of cancer, J. Med. Chem. 52 (2009) 514–523, https://doi.org/10.1021/jm801171j.
[10] H.E. Bryant, N. Schultz, H.D. Thomas, K.M. Parker, D. Flower, E. Lopez, S. Kyle, M. Meuth, N.J. Curtin, T. Helleday, Specific killing of BRCA2-deficient tumours with inhibitors of poly(ADP-ribose) polymerase, Nature 434 (2005) 913–917, https://doi.org/10.1038/nature03443.
[11] H. Farmer, N. McCabe, C.J. Lord, A.N. Tutt, D.A. Johnson, T.B. Richardson, M. Santarosa, K.J. Dillon, I. Hickson, C. Knights, N.M. Martin, S.P. Jackson, G.C. Smith, A. Ashworth, Targeting the DNA repair defect in BRCA mutant cells as a therapeutic strategy, Nature 434 (2005) 917–921, https://doi.org/10.1038/nature03445.
[12] Accessed 25 December 2018; Available from: https://www.fda.gov/drugs/informationondrugs/approveddrugs/ucm592357.htm.
[13] Accessed 27 December 2018; Available from: https://www.fda.gov/drugs/informationondrugs/approveddrugs/ucm548487.htm.
[14] Accessed 30 December 2018; Available from: https://www.fda.gov/drugs/informationondrugs/approveddrugs/ucm603997.htm.

[15] Accessed 27 February 2019; Available from: https://www.fda.gov/Drugs/InformationOnDrugs/ApprovedDrugs/ucm623540.htm.
[16] V.M. Loh, X.-L. Cockcroft, K.J. Dillon, L. Dixon, J. Drzewiecki, P.J. Eversley, S. Gomez, J. Hoare, F. Kerrigan, I.T.W. Matthews, K.A. Menear, N.M.B. Martin, R.F. Newton, J. Paul, G.C.M. Smith, J. Vile, A.J. Whittle, Phthalazinones. Part 1: the design and synthesis of a novel series of potent inhibitors of poly(ADP-ribose) polymerase, Bioorg. Med. Chem. Lett. 15 (2005) 2235–2238, https://doi.org/10.1016/j.bmcl.2005.03.026.
[17] X.L. Cockcroft, K.J. Dillon, L. Dixon, J. Drzewiecki, F. Kerrigan, V.M. Loh, N.M.B. Martin, K.A. Menear, G.C.M. Smith, Phthalazinones 2: optimisation and synthesis of novel potent inhibitors of poly(ADP-ribose)polymerase, Bioorg. Med. Chem. Lett. 16 (2006) 1040–1044, https://doi.org/10.1016/j.bmcl.2005.10.081.
[18] A. Chen, PARP inhibitors: its role in treatment of cancer, Chin. J. Cancer 30 (2011) 463–471, https://doi.org/10.5732/cjc.011.10111.
[19] D.V. Ferraris, Evolution of poly(ADP-ribose) polymerase-1 (PARP-1) inhibitors. From concept to clinic, J. Med. Chem. 53 (2010) 4561–4584, https://doi.org/10.1021/jm100012m.
[20] G.D. Zhu, J. Gong, V.B. Gandhi, X. Liu, Y. Shi, E.F. Johnson, C.K. Donawho, P.A. Ellis, J.J. Bouska, D.J. Osterling, A.M. Olson, C. Park, Y. Luo, A. Shoemaker, V.L. Giranda, T.D. Penning, Discovery and SAR of orally efficacious tetrahydropyridopyridazinone PARP inhibitors for the treatment of cancer, Bioorg. Med. Chem. 20 (2012) 4635–4645, https://doi.org/10.1016/j.bmc.2012.06.021.
[21] L. Wang, F. Liu, N. Jiang, W. Zhou, X. Zhou, Z. Zheng, Design, synthesis, and biological evaluation of novel PARP-1 inhibitors based on a 1H-thieno[3,4-d] imidazole-4-carboxamide scaffold, Molecules 21 (2016), https://doi.org/10.3390/molecules21060772.
[22] J.M. Dawicki-McKenna, M.F. Langelier, J.E. DeNizio, A.A. Riccio, C.D. Cao, K.R. Karch, M. McCauley, J.D. Steffen, B.E. Black, J.M. Pascal, PARP-1 activation requires local unfolding of an autoinhibitory domain, Mol. Cell 60 (2015) 755–768, https://doi.org/10.1016/j.molcel.2015.10.013.
[23] G. Giannini, G. Battistuzzi, L. Vesci, F.M. Milazzo, F. De Paolis, M. Barbarino, M.B. Guglielmi, V. Carollo, G. Gallo, R. Artali, S. Dallavalle, Novel PARP-1 inhibitors based on a 2-propanoyl-3H-quinazolin-4-one scaffold, Bioorg. Med. Chem. Lett. 24 (2014) 462–466, https://doi.org/10.1016/j.bmcl.2013.12.048.
[24] N.V. Malyuchenko, E.Y. Kotova, O.I. Kulaeva, M.P. Kirpichnikov, V.M. Studitskiy, PARP1 Inhibitors: antitumor drug design, Acta Nat. 7 (2015) 27–37.
[25] C. Thomas, V. Kolenko, A.V. Tulin, K. Golovine, K. Pechenkina, P. Makhov, Y. Ji, E. Kotova, A.D. Pinnola, N. Lodhi, Non-NAD-like poly(ADP-Ribose) polymerase-1 inhibitors effectively eliminate cancer in vivo, EBioMedicine 13 (2016) 90–98, https://doi.org/10.1016/j.ebiom.2016.10.001.
[26] M. Javle, N.J. Curtin, The role of PARP in DNA repair and its therapeutic exploitation, Br. J. Cancer 105 (2011) 1114–1122, https://doi.org/10.1038/bjc.2011.382 www.bjcancer.com.
[27] DNA repair in cancer therapy. Molecular targets and clinical applications, second ed., Academic Press, Elsevier, Cambridge, MA, USA; 2016.
[28] S.H. Hussien, Reduction of pyridine dicarboximide as a facil rout to synthesis of isomeric pyridine lactones, TJPS 14 (2009) 81–85.
[29] S. Sekar, N. Naik, S.A. Mahalingappa, S.K. Peethamber, Synthesis and pharmacological evaluation of certain schiff bases of octahydro-1H-pyrrolo [3, 4-b] pyridine derivatives, Int. J. Pharm. Pharm. Sci. 7 (2015) 3–10.
[30] A. Daina, O. Michielin, V. Zoete, SwissADME: a free web tool to evaluate pharmacokinetics, drug-likeness and medicinal chemistry friendliness of small molecules, Sci. Rep. 7 (2017) 42717, https://doi.org/10.1038/srep42717.
[31] K. Inoue, T. Sugaya, T. Ogasa, S. Tomioka, A facile synthesis of substituted 5–11-dihydro[1]benzoxepinol[3,4-b]pyridines, Synthesis 1997 (1997) 113–116, https://doi.org/10.1055/s-1997-1503.
[32] S.C. Karcher, S.A. Laufer, Aza-analogue dibenzepinone scaffolds as p38 mitogen-activated protein kinase inhibitors: design, synthesis, and biological data of inhibitors with improved physicochemical properties, J. Med. Chem. 52 (2009) 1778–1782, https://doi.org/10.1021/jm801291f.
[33] Chemical Computing Group; Available from: https://www.chemcomp.com/.